

DEVELOPMENT OF THE MOULD SLAG FILM AND ITS IMPACT ON THE SURFACE QUALITY OF CONTINUOUSLY CAST SEMIS

**Bridget Stewart, Neil Jones, Keith Bain, Mike McDonald,
Robert Burniston, Mick Bugdol & Vince Ludlow**
Corus Research, Development & Technology, United Kingdom

ABSTRACT

It is accepted that the majority of surface defects in the continuous casting process originate at, or within 25 mm of, the meniscus in the mould. One major influence at the meniscus and down the mould is the performance of the mould flux in terms of its melting, lubrication, solidification and transformations. The formation of slag film between the solidifying shell and the copper mould plate is critical in terms of lubrication and heat transfer, both of which are influenced by its thickness and degree of crystallisation. The films are usually only two to four millimetres thick, but the temperature difference between one face and the other can be 950°C. Varying the glass/crystalline ratio of the solid part of this film, has a significant and important effect on lubrication, heat transfer and thereby surface quality. This paper describes current and recent work to understand the role of mould slag and slag film in the surface quality of continuously cast semis within Corus UK. The work includes industrial trials to monitor powder performance on the Corus Scunthorpe Slab Caster and the development of an understanding of the crystalline phases and layers generated within the slag films through optical and electron microscopy of the slag films obtained. Two different mechanisms for the build-up of the slag film are presented. The need to understand why the same mould flux can solidify in different ways has also been identified from the samples obtained and approached using thermodynamic modelling.

INTRODUCTION

A target of all continuous casting operators is the ability to cast all grades free of surface defects. Mould powders are key to the control of initial solidification and optimisation of mould operations. The powders are fed onto the surface of the molten steel, whereupon they begin to melt, forming first a sinter layer then a mushy layer and eventually a liquid flux pool. Liquid slag from this pool infiltrates the gap between the mould and newly solidified strand. Some of this lubricates the newly-formed steel shell. However, most of the liquid freezes against the water-cooled copper mould, to form a slag film, which may crystallise over time. The phase transformations in the film are critical to the rate of heat transfer from steel to mould. The aim of the mould powder investigator is to tune the powder properties to suit the casting conditions and steel type. Industrial trials and laboratory studies involving the characterisation of mould powder behaviour, slag films, slag rims and surface quality are being carried out at Corus UK. Much of this is part of a collaborative project funded by the European Research Fund for Coal and Steel [15].

INITIAL DEVELOPMENT OF SLAG FILM

Evidence from Industrial Trials

A major part of the work on slag film development is industrial trials on the recently enhanced [1, 10] Corus Scunthorpe Slab Caster. This machine has two strands and casts carbon steel slabs up to 1970 mm wide and 235 mm or 305 mm thick at speeds of up to 1.05 m/min and 0.63 m/min respectively. Casting temperatures are typically in the region of 1550°C. The tools and techniques available for the development of mould powders at Corus [4] include mould thermal monitoring (MTM), in-mould observations, monitoring of mould powder consumption, plate dips and 'nailboards' for measurement of liquid slag pool depth, use of inclinometers for mould taper measurements during casting and laboratory characterisation of mould powders and fluxes using high temperature thermal analysis and viscometry techniques. To date twenty trials have been carried out, with eight different mould powders, A to H. This paper will focus on the trials with Powders B, C and E because of the particular information obtained from these trials regarding the initial development of the slag film.

The starting point for proposing the first mechanism of slag film development in the early stages of a casting sequence, was observations made during Trials 13 and 14, cast using Powder E. Details of Powder E are given in Table 1. During Trial 13, the mould was being observed when, after just forty-four minutes, casting was terminated prematurely. As the steel was drained from the mould, it was observed that there were large holes in the slag film at one of the narrow faces. These holes were approximately 50 mm long, 20 mm wide and were interlinked with strands of slag film, giving the film the appearance of lace netting or chicken wire mesh. These 'nets' of slag film were possibly similar to the 'rails' of film reported by Linez for billet casting. The holes were orientated with the longest dimension vertical and were of a tear drop/lozenge shape. It was not possible to see whether the slag films on the other mould plates of the same mould or of the mould on the other strand displayed the same structure. Casting of the remaining ladles had to be rescheduled, resulting in the two ladle sequence, Trial 14. During the termination of casting for Trial 14, it could be seen that the slag film was continuous.

Table 1: Approximate average powder compositions based on supplier's information

	Powder B	Powder C	Powder E
CaO/SiO ₂	1.17	0.94	1.16
SiO ₂	32.5	36	32.5
CaO+MgO	38.5	35	37.5
Al ₂ O ₃	5.25	4.25	5
Na ₂ O+K ₂ O	5.25	6.5	4.25
Fe ₂ O ₃	1.25	1.25	1.25
MnO	<0.2	<0.2	4.5
C _{free}	4.75	6.5	5
F	5	5.25	8.25
Viscosity at 1300°C	2.7	3.8	2.7

In order to determine whether a 'net'-like slag film of the type observed in Trial 13 would have existed in the early stages of Trial 14, transverse slices of the as-cast slabs were investigated in detail. Metallographic analysis was used to determine the shell development profile, surface quality in terms of longitudinal and transverse cracking and the nature of the oscillation marks. It was found that shell thinning was present, and occurred more in samples from Trial 13 and the first ladle of Trial 14 than in the samples from the second ladle of Trial 14. It could be inferred from these results that the slag film in the first ladle of Trial 14 was in a similar condition to that in Trial 13, but became more uniform during the casting of the second ladle. It would be expected that as the slag film becomes more uniform, control of heat transfer improves and a more uniform steel shell will develop.

If it is assumed that the slag film in the first ladle of Trial 14 was indeed in a similar condition to that in Trial 13, then since the slag film observed at the end of the second ladle of Trial 14 was observed to be continuous, it follows that the slag film must become continuous at some point during casting of the second ladle. In order to determine just how long it takes for the film to become continuous, the heat transfer to the mould cooling water, ΔT , and mould thermal monitoring (MTM) thermocouple temperatures have been analysed.

Analysis of the mould water ΔT values shows that in Trial 13, ΔT is still increasing when the cast is stopped after 44 minutes. An explanation for the increase in ΔT with time is proposed below. Where the slag film is present, heat transfer from the steel strand to the mould will be high. Where there is no slag film, i.e. in the 'holes', the shell and mould will be separated by an air gap and heat transfer will be much lower. Hence as the holes become filled with slag, the heat transfer to the mould will increase, leading to an increase in ΔT . Once complete coverage has been achieved, the slag film will start to get thicker and heat transfer will decrease. Thus, all other casting parameters being equal, it could be expected that the point at which the slag film becomes complete, corresponds to the maximum value of ΔT . In this case, sixteen minutes into the second cast. Hence it has taken eighty minutes from the start of casting for a complete slag film to form. In the meantime, the heat transfer conditions 'seen' by the strand on travelling through the mould could be expected to have been very variable. Although the temperature signals from the MTM system show some reduction in variability after ninety minutes, the improvement is not a marked one.

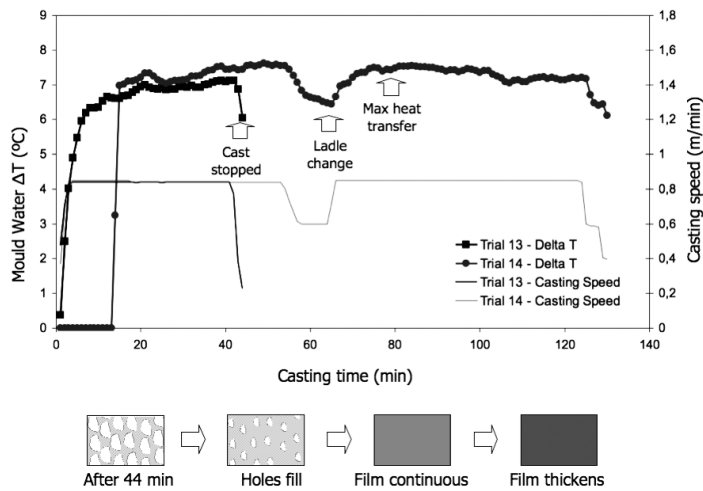


Figure 1: Increase in mould water temperature for narrow plates observed in Trials 13 and 14 and schematic showing corresponding development of slag film with time

The amount of cracking found on the samples was very limited and there was no evidence to suggest that one sample was worse than another. All the narrow face samples displayed a degree of very fine network, or spongy, type cracking. Maximum crack depths were around 0.5 mm. Mould slag infiltration may be expected to influence oscillation mark formation. The oscillation marks observed were mainly hook-type but there were some fold-type marks present. There was no clear trend in the oscillation mark formation type from cast-to-cast. These results suggest that the time taken to develop a continuous slag film from Powder E has not had a detrimental effect on the as-cast slab surface quality.

Evidence from Physical Appearance of Slag Films

The opportunity to obtain samples of mould slag films from industrial casters is critical to the success of this work. Historically slag films were obtained at British Steel/Corus UK by either dropping the mould level during casting and removing a small sample from near the meniscus, removing slag rim samples from the mould with some slag film attached or catching fragments in a wire basket placed below the mould. However, due to the findings that most defects originate at or near to the meniscus, removal of slag films and slag rims from the mould is no longer permitted during casting. Also, the new safety enclosure around the strand below the mould exit, makes it difficult to collect film fragments as they fall out of the bottom of the mould. More recently Corus have followed the example of O'Malley and Neal [12], Hooli [6, 7] and Bezerra [2]. By catching the slag film as it falls off the mould walls during 'cap-off' or 'tail-out', it has been possible to obtain a significant amount of material. Although no film samples could be obtained at the cap-off of Trials 13 and 14 described above, large samples have been obtained for trials of other powders. The films have been characterised using a variety of techniques and the results obtained could help in understanding the mechanisms of slag film development.

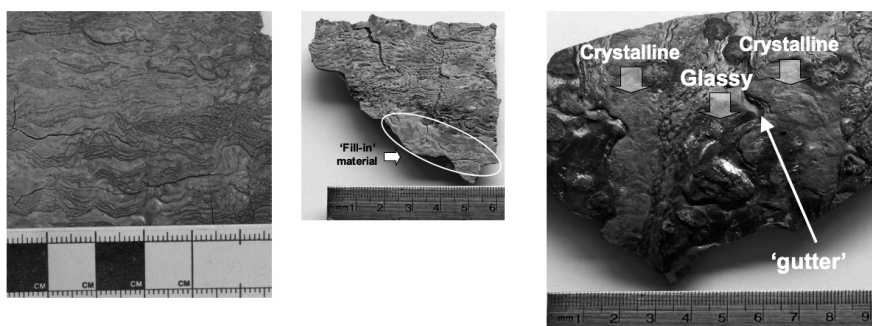


Figure 2: Slag film surfaces that had been in contact with mould, obtained from Corus Scunthorpe Slab Caster at the end of (a) Trial 4, Powder C (b) Trial 7, Powder C and (c) Trial 6, Powder B

The first stage of slag film characterisation was visual inspection. It was immediately obvious that there were considerable differences between slag films generated by different powders and also between films generated by the same powder in different sequences. The surfaces which had been in contact with the mould were very smooth [14, 15]. Of particular interest for understanding the development of these slag films were the features revealed when the surfaces which had been in contact with the mould were examined. Figures 2a and 2b show the 'mould-face' of Powder C films obtained from two different trials with casting times of 2 hr 52 min and 4 hr 39 min respectively. In both cases it can be seen that the surface has folded as the material has been pushed down the mould. In Figure 2b it can be seen that the surface in contact with the mould has started to break up and fresh liquid slag has filled the cracks formed. It is expected that the folds or 'ripples' are related to the mould oscillation and will lead to air gaps between the film and mould wall. However, in this case the folds are relatively small and evenly distributed.

Hooli [7] has recently reported very similar patterns of surface roughness in slag films obtained after casting stainless steel slabs. He has attributed these 'wavy lines' to poor wetting of the liquid slag on the mould face such that the slag attempts to avoid spreading. Spreading then becomes a forced phenomenon which can happen during the downward motion of the mould. According to Hooli, this explanation is only valid for the first layer in the mould and therefore involves the claim that the rippled areas of the slag films obtained at 'cap-off' must have persisted from the start of casting. In the Corus film in Figure 2b, it is interesting to note that the material that filled the fractures in the film after the start of casting, has formed a much smoother surface, although some ripples are present, suggesting that either the ripples cannot fully form after the start or that they take a long time to develop during casting.

Examination of the mould face surface of Powder B films, reveals a very different situation. A typical example, taken at the end of 8 hr 31 min casting, is shown in Figure 2c. There appear to be vertical stripes of crystalline material, with stripes of glassy material in between. Moreover, it would appear that the glassy material is not always in contact with the mould, rather it forms gutters approximately 13 mm wide and up to 1 mm deep. The nature of this surface roughness suggests that the Powder B slag film was not all formed at the same time, but rather that 'stripes' of slag film formed first and the gaps in between were later filled in with liquid slag which was in full contact with the strand, but only partial contact with the mould. This type of slag development is similar to that suggested above for Powder E. When mould water temperature increases, ΔT were plotted against casting time for Powder B films, it was seen that, as with Powder E, ΔT increases throughout the first ladle, peaks during the second ladle and continues to

decrease during subsequent ladles. Unfortunately analysis of the ΔT values for Powder C films indicate that more trials are needed to identify trends.

It is known from studies of the compression of rock layers in the earth's crust, that the thinner the layer being compressed, the greater the number of ripples formed [3]. The depth of the air gap channels is expected to have a significant influence on the thickness of the slag film. The differences observed here between the films from Powder B and C may go some way to understanding the variation in the range of film thickness observed by Ludlow *et al.* in fragments obtained below the mould [11].

UNDERSTANDING DEVELOPMENT OF LAYERS WITHIN SLAG FILM

Hooli has published some very interesting work on the characterisation of slag films using electron microscopy [5, 6], describing how the layers of slag film build up over time, porosity develops and the slag film breaks up and drops out of the mould. The existence of five layers within the films was reported:

- A layer formed during 'tailout' or 'cap-off'
- A thin layer on the strand shell side, which was possibly the liquid lubricating layer
- A layer with high calcium content
- A layer with high aluminium content with pores
- A layer with high sodium and fluorine content as a first layer against the mould.

In the current work, Corus have carried out similar measurements to determine whether the same is true for slag films taken from their plants.

Characterisation of Element Distribution in Corus Slag Films

Hooli measured the composition of his samples at 100 μm intervals along a line through the thickness of the films using Scanning Electron Microscopy and EDS analysis. The five layers reported were visible in a plot of chemistry against distance from the mould face. In the current work, SEM/EDA analysis was used to determine the composition of 50 μm x 50 μm areas at 50 μm intervals through the thickness of the films.

The plots for the Powder C films were all very similar and an example obtained for a Trial 4 film can be seen in Figure 3. The key features are:

- A relatively high degree of variability in calcium content; up to 10 wt% over 150 μm
- Below approximately 800 μm from the mould wall, the fluorine content increases
- Alumina content peaks at approximately 800 μm from the mould wall
- The sodium content loosely mirrors the alumina content. It is highest in the region closest to the mould and also around 800 μm from the mould wall. However, although the 'baseline' sodium levels are similar to those in Hooli's film, the step changes are not as dramatic
- A small step change in silica content at approximately 800 μm from the mould wall
- A layer at over 1550 μm from the mould wall which appears to be more homogeneous than the rest of the film, particularly with respect to calcium. This could correspond to the layer that Hooli proposes is formed during tail out or cap off or was the liquid lubricating layer when casting stopped.

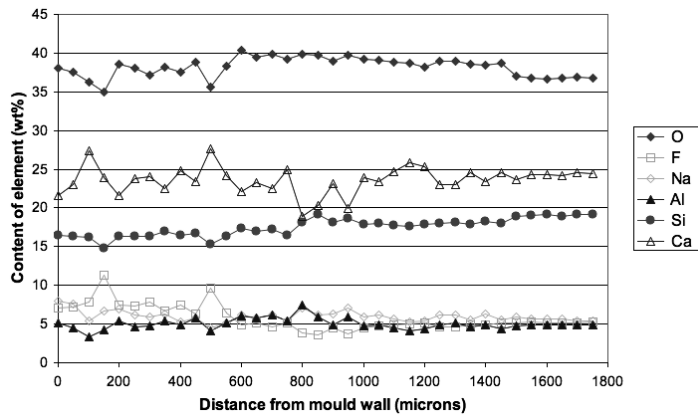


Figure 3: Contents of some elements in Corus Powder C slag films analysed with SEM/EDA

Five different trials were carried out using Powder B. Most of the films obtained showed similar variation in composition to that shown for a Trial 6 film in Figure 4a. The key features for this film are:

- The variability in calcium is much less than in the Powder C film
- The silicon content changes very little
- Changes in Na content again mirror changes in Al, but the magnitude of these changes is less than in the Powder C film
- There is some fluctuation in fluorine content and this is the mirror image of the changes in Na and Al. Fluorine is approximately 2 wt% lower close to the mould wall than at the side that had been in contact with the strand
- Beyond 2100 μm from the mould wall there is very little change in the concentration of any of the elements and this may correspond to a layer formed at 'tail out' or the liquid lubricating layer.

However, a Powder B film obtained from Trial 5, showed a very different distribution of calcium and silicon (Figure 4b). Up to 800 μm from the mould wall, the silicon content is the same as for Trial 6 film and the average calcium content is slightly higher but beyond 900 μm from the mould wall, the Ca content drops and the Si level increases, such that the contents of these two elements are very similar to each other. The reason for this is not yet clear.

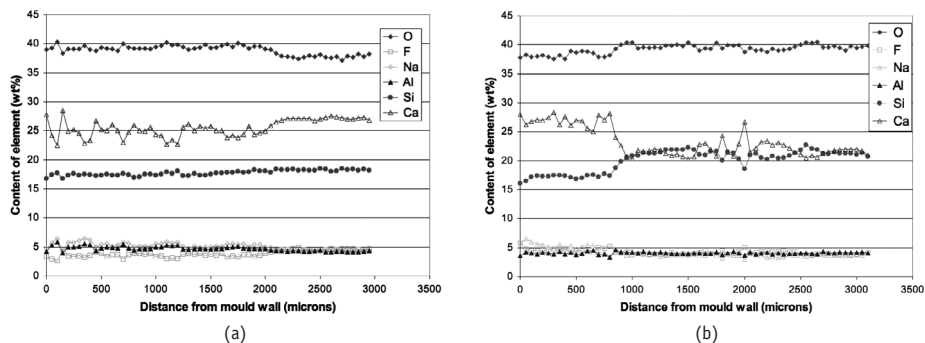


Figure 4: Contents of some elements in films which are (a) typical (Trial 6) and (b) not typical (Trial 5) for Powder B slag films obtained from Corus Scunthorpe Slab Caster

SEM/BSE Images of Slag Films

Bands or regions of crystallised phases were visible in the SEM/BSE images of all of the Corus slag films. Examples of full through thickness areas of two films are given in Figures 5 and 6 respectively. In both figures, six different points in the film have been identified and higher magnification SEM/BSE images of these areas obtained, together with chemical analyses of phases identified. For Powder B, Area 1 will have been in contact with the steel strand and Area 6 closest to the copper mould wall. For Powder C, the converse is true, with Area 1 being in contact with the mould.

Remarkably in all of the Powder B and Powder C films studied, there is a crystalline region next to the mould and a glassy region next to the strand. In the Powder B films, pores are present at the interface between the glassy and crystalline regions whereas the Powder C films contain gas bubbles near the film-mould interface. It is generally thought that when the liquid slag first enters the mould-strand gap, it is quenched against the mould wall to form a glassy layer. Then over time, due to the heat from the strand, the hotter parts of the film close to the strand starts to crystallise, to give a film with a crystalline region sandwiched between the glassy region next to the mould wall and another glassy region due to cooling of what had previously been the liquid lubricating layer. However, this is not the case for the Corus slag films and crystallinity in the film next to the mould has been reported elsewhere [13]. Watanabe has suggested that because the melting point of cuspidine is so high, there is potential for it to form between the shell and mould at very early stages of the process. Also, Li *et al.* have shown that even a temperature as low as 100°C with a holding time of 10-20 minutes is enough to influence the percentage crystallinity significantly.

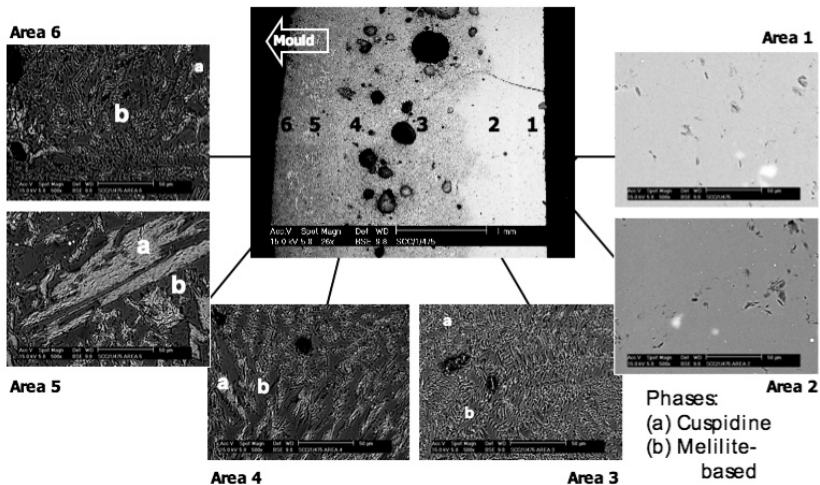


Figure 5: SEM/BSE Images of film derived from Power B (Trial 6)

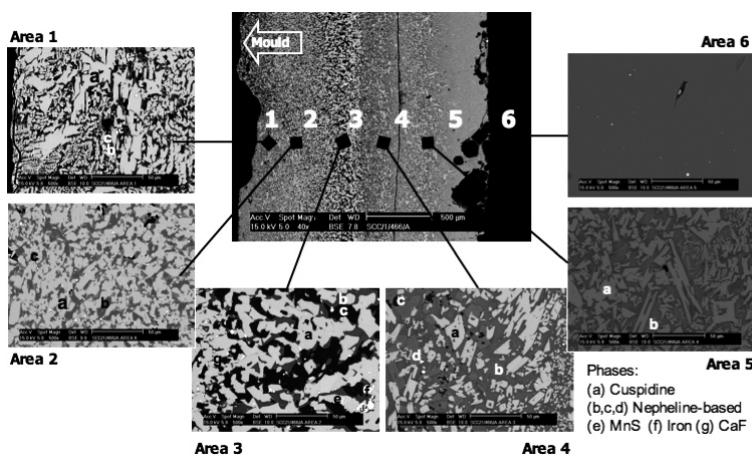


Figure 6: SEM/BSE Images of film derived from Power C (Trial 4)

Thermodynamic Study of Phase Formation

In an attempt to understand the formation of the different phases in the Corus slag films, a brief thermodynamic study was carried out, using both the full elemental SEM/EDA measured compositions as indicated by Figures 3 and 4 in conjunction with the more detailed, although more limited (fluorine analysis was only qualitatively reported) phase analysis from the SEM/BSE images given in Figures 5 and 6. Whilst accepting that the extreme cooling conditions of these films is far removed from the equilibrium state, it was thought that examining the theoretical equilibrium phase distribution and comparing this with what could be seen in the film, would give some indication of their behaviour. The thermodynamic package MTDATA was employed in conjunction with the MTOX6.1 database.

The model predictions suggest that the predicted primary precipitating phase for powder C is cuspidine ($3\text{CaO}\cdot 2\text{SiO}_2\cdot \text{CaF}_2$). This was supported by subsequent XRD analysis of the samples. The SEM results are also indicative of this result, although, due to the qualitative nature of the fluorine analysis, only the presence of a di-calcium silicate (C2S) phase with a detectable fluorine content could be confirmed. This phase was present as one of the crystallised phases in samples designated from Areas 1 to 5. However, it was not present in Area 6 even though it had been predicted from the bulk composition of Area 6. As cuspidine in Area 6 would normally have formed at about 1220°C , this suggests that the rate of cooling was sufficiently rapid to pass through the region of supersaturation without nucleating the phase. This did not occur in the other areas examined. Thus, although the cooling of the material next to the mould is not sufficiently rapid to produce a glass, it has generated different phases to those in the rest of the film. In the samples from Areas 1 to 3 two phases were identified as CaF_2 and MnS by the SEM but the remaining two phases showed that they should have been complex precipitates in the nepheline primary phase field ($[\text{CaVa}^{+2}, \text{K}_2^{+2}, \text{Na}_2^{+2}]_1[\text{Al}^{+3}]_2[\text{Si}^{+4}]_2[\text{O}^{2-}]_8$). That several phases were predicted from the SEM analyses of the identified crystal possibly suggests that both the crystallites were nepheline but the electron beam had detected variable amounts of matrix material beneath them. In all three areas the predicted start of formation of nepheline was about 1120°C , suggesting a much slower cooling regime than was found in Area 6. This slower cooling may also account for the increased crystal size of the cuspidine in these areas indicating that nucleation and suitable supersaturation of this phase was more easily achieved. Interestingly, the crystallisation in Area 4 shows a

marked difference from Areas 1 to 3. Here the nepheline crystallises as a distinct phase, leaving what appears to be a melilite type based glass matrix (a solid solution in the gehlenite – akermanite region) with some crystals of melilite being formed.

The model predictions for powder B indicated that there are effectively two primary co-precipitating phases of cuspidine and melilite, appearing at between 1210 and 1230°C and in equal amounts. Areas 1 and 2 appear to be an homogenous glassy phase whose composition indicates a rapidly cooled liquid to below this temperature. In Area 3 a slightly more complicated behaviour is observed where crystallisation appears to occur from a predominantly melilite liquid slag. Although the composition of the precipitated crystals suggests that a number of stable phases could be present at temperatures below, it is thought that the principal phase formed was cuspidine and that the remaining material analysed represents either co-precipitated melilite or the melilite based liquid from which the cuspidine precipitated. This suggestion has tentative support from the results of Area 4 where a similar microstructure is observed, however, the precipitates are significantly larger and analyse specifically as slightly SiO₂ rich C2S in the presence of fluorine. The matrix material, melilite, is almost identical to that in Area 3. Area 5, clearly shows highly developed precipitation of large ‘cuspidine’ crystals in what appears to be a matrix of rapidly solidified melilite type based slag. Area 6 shows a structure which is almost identical to Area 3, giving rise to similar results.

CONCLUSIONS AND FURTHER WORK

The Corus slag films show some similarities to but also some differences from the Outokumpu slag films reported by Hooli.

By obtaining much larger samples of mould slag film than were previously available within Corus UK, it has been possible to identify two different types of roughness in the slag film surfaces which were in contact with the mould. In order to explain these observations, two different patterns of initial slag film generation have been proposed:

- In the first case, the slag is forced into the top of the mould strand gap as a continuous layer. A thin uniform layer in contact with the mould crystallises and as further material is forced in with each oscillation of the mould, the film surface in contact with the mould is compressed to form fine ripples.
- In the second case, the slag flows more freely into the mould-strand gap, not as a continuous layer as in the first case, but as a net-like structure which holds the shell off the mould. Initially the holes are filled with air, but are gradually filled with slag. The result is a network of crystalline material with more glassy regions in between. Often these glassy regions are not as thick as the neighbouring crystalline regions.

Further work is underway to determine the implications of the two types of film for lubrication, heat transfer and as-cast surface quality.

All of the films obtained in this work exhibited a crystalline region next to the mould. A thermodynamic study has shown that for the Powder B films the rapid cooling in this area has generated different crystalline phases to those in the rest of the film. Additional thermodynamic modelling is being carried out to understand variations between films obtained from the same mould flux.

ACKNOWLEDGEMENTS

The authors would like to thank the ERFCS for their financial support of this work through Project RFSR-CT-2005-00012, the slab caster operators at the Corus plants where this work was carried out, Martyn Whitwood for SEM analysis and Neil Hunter for helpful discussions.

REFERENCES

- Barber, B. & Ludlow, V., et al.** (2008). 6th European Conference on Continuous Casting, Rimini. [1]
- Bezerra, M. C. C., Afrange, O. D. C. & Valdares, C. A. G.** (2002). Proc. Mills Symposium, p. 293. [2]
- Cosmo Caixa** Science Museum, Barcelona. (2008). [3]
- Harris, B., et al.** (2005). Proc. 5th European Conference on Continuous Casting, Nice p 66. [4]
- Hooli, P. O.** (2002). Proc. 4th European Conference on Continuous Casting, Birmingham, p. 379. [5]
- Hooli, P. O.** (2002). Ironmaking & Steelmaking, 2002, Vol. 29, No 4, p. 293. [6]
- Hooli, P. O.** (2007). PhD Thesis, Helsinki University of Technology, October 2007. [7]
- Li, Z., Thackray, R. & Mills, K.** (2004). Proc. Slags 2004, Cape Town, 2004, pp. 813-819. [8]
- Linez, E.** Private communication. [9]
- Ludlow, V. & Barber, B., et al.** (2007). SMEA Conference, Sheffield, June 2007. [10]
- Ludlow, V., Harris, B., Riaz, S. & Normanton, A. S.** (2004). Proc. Slags 2004, Cape Town, p. 723. [11]
- O'Malley, R. J. & Neal, J.** (1999). Proc. METEC Congress, Düsseldorf, pp. 188-195. [12]
- Ogibayashi, S., et al.** (1987). Nippon Steel Technical Report No. 34 July, pp. 1-10. [13]
- Stewart, B., et al.** (2006). IOM Conference on Surface Quality, London, November 2006. [14]
- Stewart, B., et al.** (2008). Proc. 6th European Conference on Continuous Casting, Rimini, p. 22. [15]
- Stewart, B., Ludlow, V., Däcker, C. Å., Glaes, M., Unamuno, I., Rödl, S., Kolm, I. & Miceli, P.** (2008). RFSR Contract RFSR-CT-2005-00012, July 2005 – December 2008. [16]
- Watanabe, T., et al.** (2000). Metallurgical and Materials Trans.B, 2000, Vol. 31B pp 1273-1281. [17]

